MINERALOGICAL MAGAZINE, VOL. 45, 1982, PP. 167–78

Porphyritic-nodular, nodular, and orbicular chrome ores from the Sakhakot-Qila complex Pakistan, and their chemical variations

ZULFIQAR AHMED*

Department of Geology, University of London, King's College, London WC2R 2LS

ABSTRACT. A new kind of chromitite texture—a porphyritic nodular texture, found in an alpine-type complex in Pakistan, is described. The chromite from phenocrystic nodules and that from their disseminated chromitite groundmass show comparable trivalent elements and postcumulus to subsolidus Mg-Fe^{2+} variations, which are also recorded from 'normal' nodular ore samples. The nodular ores differ from all other textural types of chromitite from this complex in an unusual, though slight, increase in Cr/(Cr+Al) with Mg/(Mg+Fe^{2+}) between stratigraphically different desposits, which is caused by magmatic differences. The implications of major element variations in chromites and olivines of nodular chromitites are discussed and a cumulus origin is supported. Temperatures of final chromite-olivine equilibration ranged from 750 to 900 °C, the individual nominal values being higher for chromitite with coarser chromite crystals and, or, higher chromite: silicate ratio.

NODULAR and orbicular textures are a characteristic feature of podiform chrome ore deposits and help distinguish them from stratiform deposits (Thayer, 1969; Dickey, 1975). They are significant not only as a peculiar type of texture but also as evidence of distinctive petrogenesis of alpine-type ultramafic rocks. In earlier works, e.g. Thayer (1960, 1969), Kaaden (1963), Leblanc (1980), and Cassard *et al.* (1981), the role of textures of chrome ore has been stressed in appraising theories of their origin, as the original crystallization relations are best preserved in them. Genesis of nodular and orbicular textures has long been controversial (Thayer, 1969; Dickey, 1975; Greenbaum, 1977; Leblanc, 1980). In this communication a new occurrence of chromitites with predominant nodular texture and a 'porphyritic nodular' texture is described. Chemical variations in minerals of such textural varieties are outlined and interpreted. Olivine-spinel geothermometric methods are used to assess their re-equilibration conditions.

* Permanent address: Institute of Geology, University of the Punjab, New Campus, Lahore, Pakistan.

Geology of the chromite deposits

The chromite deposits occur in the Sakhakot-Qila ultramafic complex, Malakand Agency, Pakistan, which is an ophiolite segment tectonically emplaced in its present location (Ahmed and Hall, 1981, fig. 1). In its overall aspect the complex is of alpine-type and broadly conforms to the harzburgite subtype of Jackson and Thayer (1972). It is composed mainly of harzburgite (65%) and some wehrlite (25%); both enclose minor bodies of dunite (8%). In these three rock types, up to 10 modal per cent chromite is considered accessory (Thayer, 1970), and is ubiquitous. Higher modal chromite constitutes 'chromitites', which are usually found enclosed in dunite, and rarely wehrlite. Younger dykes of pyroxenite cut across all other ultramafic rock types, and are in haphazard orientation. Still younger dykes and lenses of rodingite are present in higher concentration towards the northern contact of the ultramafic rocks with metagabbro (fig. 1). This metagabbro has three smaller outcrops towards the north, the stratigraphic top, of the complex (called 'gabbroic rocks' in fig. 1). Dolerite dykes occur at two locations in the upper part of the ultramafic sequence, and apparently lie below the gabbro. At one location these dykes are metasomatized and cut by white grossular veins.

The chrome-ore mines and outcrops located during the recent detailed mapping show that chromite deposits are present at sixty-two locations, as shown in fig. 1, and are concentrated in a smaller zone within ultramafic rocks, here called the 'chromitiferous zone'. This zone runs parallel to the east-west elongation of the complex. A stratigraphic zonation of the chromitiferous zone roughly parallel to its elongation has been recognized (Ahmed and Hall, 1981) on the basis of (i) shape and extent of chromitite bodies, (ii) chromitite textures, and (iii) Cr/Al contents of unaltered chromites. Deposits towards the south in fig. 1 are

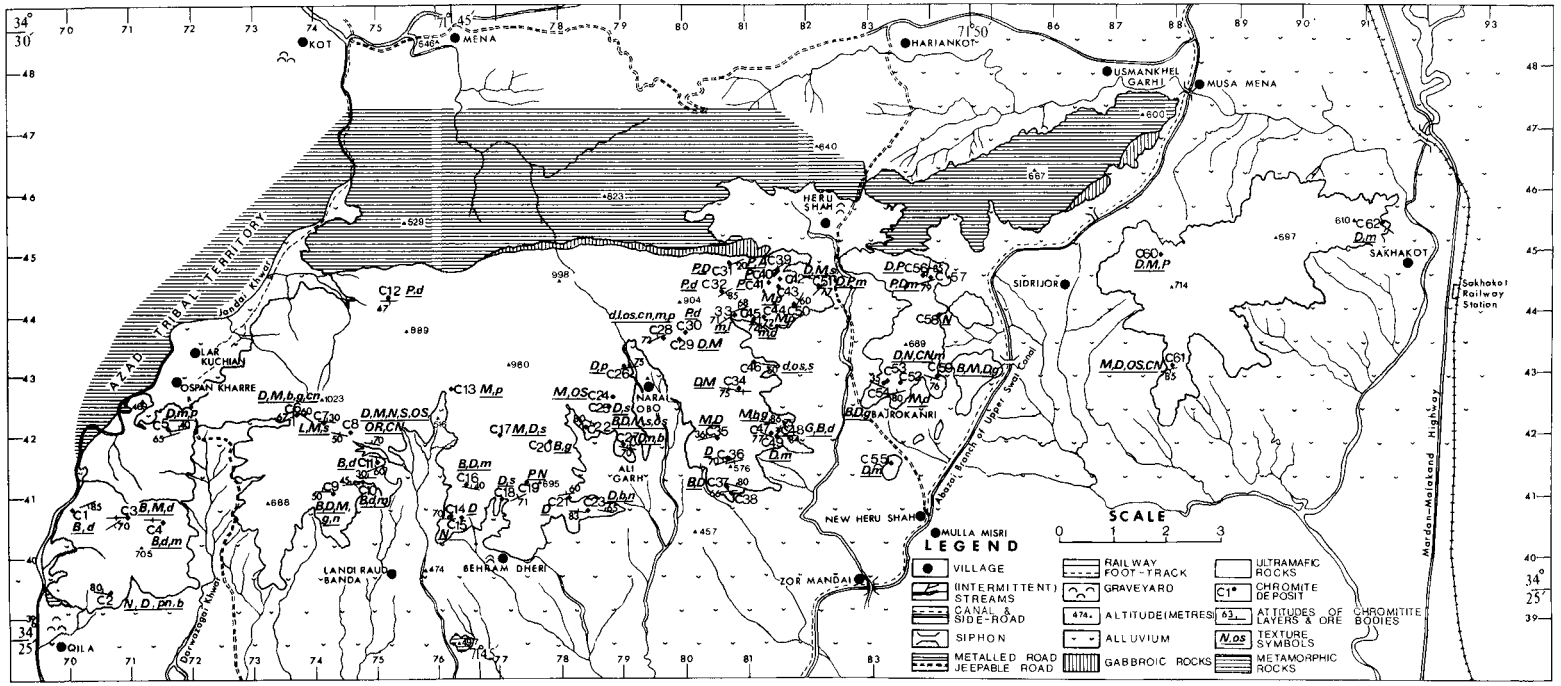

FIG. 1. Map showing locations of chromite deposits (C1 to C62) and geology of the Sakhakot–Qila complex, Pakistan. The complex is in tectonic contact with outer metamorphic rocks. The chromitite textures at each deposit are displayed by oblique symbolic letters, written in order of decreasing abundance. In addition, the capital letters denote prevalence or abundance, and small letters show a lesser development.

DECREASING OVERALL ABUNDANCE ▼

TEXTURE	SYMBOLS
D, d	DISSEMINATED
B, b	SCHLIEREN BANDED OR REGULARLY LAYERED
M, m	MASSIVE
P, p	PSEUDO-CLASTIC
N, n	NODULAR
CN, cn	CHROMITE NET
S, s	SPECKLED
OS, os	OCCLUDED SILICATE
L, l	LENTICULAR BANDED
G, g	GRADED LAYERED
PN, pn	PORPHYRITIC NODULAR
OR, or	ORBICULAR
A, a	AUGEN DISSEMINATED

generally more layer-like ore bodies with considerable lateral extensions, although lenticular ore bodies are also present. They have 'high-Cr' chromites. Deposits towards the north have 'high-Al' chromites, and their ore bodies are typically podiform to dyke-like and are usually of a smaller size although the modal chromite is usually high.

Chromitite textures

The chromitites were thoroughly sampled, and specimens showing different types of chromitite textures were collected. The hand specimens and their sawn surfaces revealed various textural varieties whose provenance at all the deposits is shown in fig. 1. The deposits with schlieren-banded and graded-layered textures occur in an east–west trending belt in the southern part of this chromitiferous zone. Here, the lateral ore bodies are generally most persistent. In the northern deposits, apart from the disseminated and massive textures that are prevalent everywhere, a clastic-looking texture occurs composed of rounded to subrounded chromite grains of coarse to very coarse size (up to 2.5 cm across) and have bluish-grey chlorite as matrix or halos around chromite grains. The texture is here called 'pseudoclastic'.

Nodular and related textures

The distribution of nodular and related textures in fig. 1 shows that they are dominantly developed south of the belt of banded ores. The porphyritic nodular ore is confined to this part. North of the banded ores, the orbicular and nodular ores are both developed in adjacent ore bodies at C8. At C53, layers of nodular and chromite net ores lie in contact with each other. Further north, nodular ore is developed at C58.

Nodular texture. 'Nodular ore' has been the most widely adopted of many synonyms, e.g. spherical ore, globular ore, egg ore, ovoids, grape ore, bean ore, leopard ore, and shot ore. The nodular chromitites are rounded to elliptical aggregates of chromite crystals; the nodules are set in a silicate matrix, and occur characteristically in only the podiform deposits (Thayer, 1960, 1964, and 1969). The nodules can be classified as: (i) massive: unzoned nodules of dense aggregates of coarse chromite crystals (e.g. fig. 2B); (ii) cored: nodules with a core of intergrown chromite and silicates, and an outer rim of more massive chromite (e.g. Thayer, 1969, fig. 9; Greenbaum, 1977, fig. 5; Pavlov *et al.*, 1977); (iii) silicate-rich: nodules, usually unzoned, with appreciable silicates intergrown with chromite (e.g. fig. 2A); (iv) broken: nodules intersected by silicate-filled cracks, which, if absent, would give typical solid nodules.

In the Sakhakot–Qila complex, the nodular ore is prevalent at the following deposits shown in fig. 1: C2, C8, C9, C15, C23, C53, and C58. Among these localities, and among individual ore bodies of single deposits, e.g. C8, the nodules exhibit differences in their size, closeness of packing, chromite–silicate relations, and tectonic effects (fig. 2). Nodule shapes are usually spherical, rarely elliptical, and in the latter case may be oriented. Nodules may be in point contact with each other, as in fig. 2B, or widely separated, as in fig. 2C (cf. Greenbaum, 1977). Cored nodules, comparable with those of Troodos complex (Greenbaum, 1977) or Camagüey, Cuba (Thayer, 1969), have not been found in the Sakhakot–Qila deposits. However, less spherical but rounded nodules intergrading into large 'crystals' as illustrated by Thayer (1969, fig. 7) are present at C58.

Orbicular texture. This comprises spherical units, the orbicules, each of which consists of a nucleus, an aggregate of chromite crystals, surrounded by a rim of partly serpentinized olivine which, in turn, is surrounded by a matrix of chromite (Johnston, 1936; Thayer, 1969; Bilgrami, 1964; Shams, 1964; Mukherjee, 1969). Variations have been reported in which orbicules may be composed of several chromite layers (Johnston, 1936; Greenbaum, 1977); the nuclei may be absent or the orbicules may be oriented. The orbicular ores of the Sakhakot–Qila complex are developed only at the Landi Raud deposit (C8) which is the biggest deposit and is enclosed in the biggest dunite body of the complex. Here it occurs at the same chromite horizon which contains the nodular ore (cf. Greenbaum, 1977). The 'orbicule nuclei' are thick spheres of almost pure coarse-grained chromite, average ~ 1 cm across. They are surrounded by dunitic shells without chromite, here called 'orbicule mantles', which are enclosed in the 'orbicule rims' of fine-grained chromite and olivine, and which outline the orbicules and fill interstices.

Porphyritic nodular texture. This texture has not been identified before, and is typically developed at two deposits, numbered C19 and C2 in fig. 1. It is an inequigranular texture in which typical nodules of variable, sometimes similar, size occur embedded in a matrix of typical 'disseminated' chromitite, with finer-grained chromite. The nodules are similar to those of 'normal' nodular ores. A typical specimen is illustrated in fig. 2F. Nodules exceeding 3 cm in diameter are not uncommon at C19 deposit where they show seriate variation to finer sizes below 5 mm diameter and no evidence of compaction or deformation under load. The term 'disseminated' chromite, as used here, is not synonymous with 'accessory' chromite as has been implied by Greenbaum (1977) but

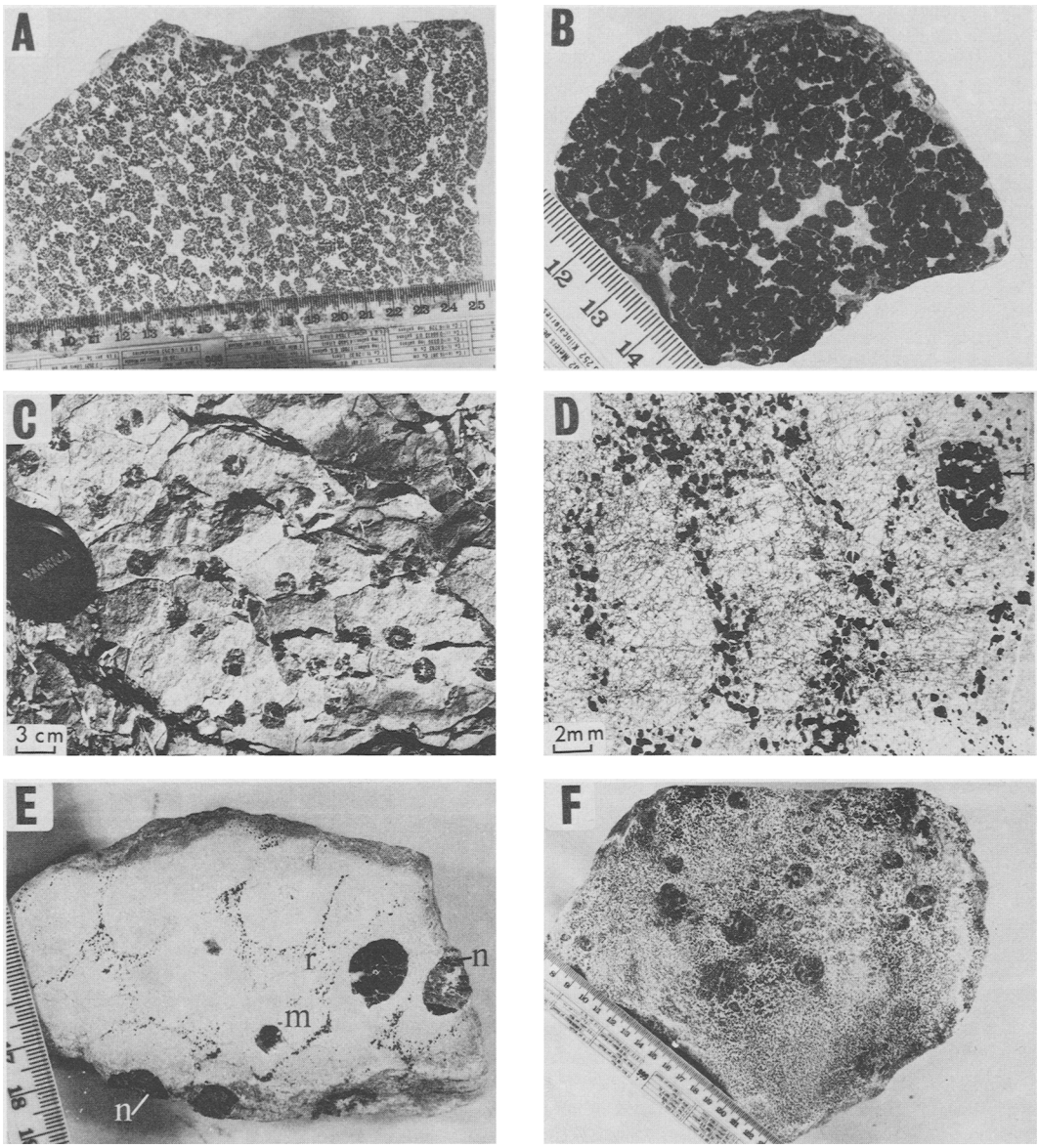

FIG. 2. (A) Specimen of nodular ore from the Landi Raud deposit (C8 in fig. 1) showing silicate-rich elongated nodules that contrast with the spherical nodules from the same deposit shown in (B) and (C). The nodules are not 'cored' and the primary silicate inside and outside the nodules is highly magnesian olivine whose grains may be optically continuous across the nodule boundaries. (B) Specimen with closely spaced, spherical 'solid' nodules from C8. (C) 'Solid' spherical nodules with very low chromite : silicate ratio, from a quarry face at C8. (D) Projection microscope photograph of chromite net ore of cumulus origin (Thayer, 1969), with a chromite nodule (n) grown as nucleus of an olivine oval. Sample no. Z257 from C53. (E) Orbicular chromitite sample showing orbicule 'nuclei' (n) resembling the nodules of nodular ores; surrounded by olivine 'mantles' (m). The orbicule 'rims' (r) form a chromite net texture. Sample no. Z72 from C8. (F) A sawn surface of porphyritic nodular ore, sample no. Z150 from C19, showing various-sized nodules embedded in the disseminated high-grade chromitite. The specimen is treated with HF to whiten olivines; chromite is black.

denotes relatively fine-grained single crystals of chromite scattered more or less homogeneously in the host silicates. Usually the modal chromite ranges from 40 to 80%.

Chemical composition

The chromite and adjacent olivine grains in samples from different deposits of the complex were analysed by a Cambridge Instruments Microscan electron-probe microanalyser operated at 15 kV accelerating potential and 100 live seconds counting time, and fitted with a Si(Li) detector and a Link Systems energy-dispersive system. Cobalt was used as internal standard and ZAF corrections applied through an on-line computer. The spots analysed were selected away from the altered parts of the grains which are easily distinguishable optically. The inter-grain inhomogeneity was below the analytical error.

The chromite nodules lack zoning as portrayed in previous studies on nodular ores, e.g. Thayer (1964, 1969), Snelgrove and Ruotsala (1968), Dickey (1975), and Greenbaum (1977). The representative chromite analyses are listed in Table I. Overall, the primary chromites fall in the 'aluminian spinel' and 'chromian spinel' fields of Stevens (1944) and some plot in his metallurgical grade. The chromites show a strong chemical resemblance to the podiform-type chromite deposits of the world, according to the compositional criteria defined by Thayer (1964, 1970), Irvine (1965, 1967), and Dickey (1975). The plot of the spinel compositional prism for nodular and related ores, after the method of Irvine (1965) is given in fig. 3A. The nodule-making coarser chromite crystals are plotted with solid symbols, and the finer grains outside the chromite nodules in more olivine-rich parts of the samples are plotted with open symbols. Both types of plots representing individual deposits are joined by arrow lines. The plot shows that the $Mg\text{-}Fe^{2+}$ substitution is quite small compared with the Cr–Al substitution. The nodular ores of this complex are frequently of high-Cr type and rarely of high-Al type. Between the deposits, $Mg/(Mg+Fe^{2+})$ and $Cr/(Cr+Al)$ show sympathetic variation in the nodule-making chromites (solid symbols in fig. 3A) and this deviates from the non-nodular chromitites from this district, in which either an antipathetic variation is noticed, or $Mg/(Mg+Fe^{2+})$ remains constant with changes in $Cr/(Cr+Al)$. Thus, in fig. 3B, the field of segregated chromites based on 1000 microprobe analyses from both nodular and non-nodular ore samples from this complex shows a different trend. The field of accessory chromites shows even more antipathetic relationship between the two variables.

The chromites within individual deposits do not show strong variations like those encountered between the deposits. Also, within deposits, the $Mg\text{-}Fe^{2+}$ substitution is quite large compared with the Cr–Al variation. In each sample the coarser and finer chromite components vary only in $Mg\text{-}Fe^{2+}$, and show negligible or overlapping variations in their trivalent cations. Analyses from such components are listed separately in Table I.

Among the porphyritic nodular ores, plotted towards the Cr-rich part of fig. 3A, the chromite crystals forming the phenocrystic nodules and the chromite-rich disseminated ore, forming the matrix, show consistent differences in Mg and Fe^{2+}

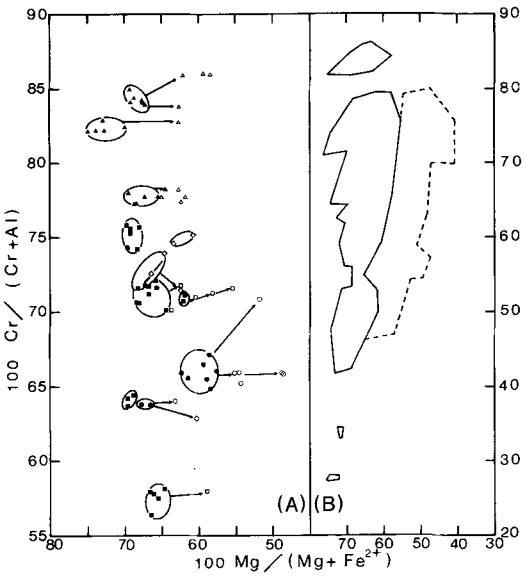

FIG. 3. (A) $Cr/(Cr+Al)$ *vs.* $Mg/(Mg+Fe^{2+})$ plot (after Irvine, 1965) for chromite grains composing nodular and related ore textures of the Sakhakot-Qila complex. The ellipses enclose analyses from individual deposits for only the coarser chromites (solid symbols) which show, between the deposits, a slightly sympathetic variation between the above variables. Arrow-lines point to finer chromites at each deposit, and may indicate postmagmatic and subsolidus re-equilibration trends. (B) Field of 1000 electron microprobe analyses of segregated chromites, enclosed by solid line, and adjacent field of 200 analyses of accessory chromites shown by broken line, from various deposits of Sakhakot-Qila complex. Porphyritic nodular ores: ▲ coarse nodule-forming chromite; △ disseminated chromite. Nodular ores: ■ coarse chromite of solid nodules; ◆ chromite of silicate-rich nodules; □ ◇ fine, accessory chromite in dunitic matrix of the nodules. Orbicular ores: ● coarse chromite of the 'orbicule centres'; ○ fine chromite of the 'orbicule rims'.

Table I. Representative chromite and adjacent olivine analyses from samples showing nodular and related textures.

Texture	Porphyritic nodular						Nodular											Orbicular			
Deposit & Sp.No.	C2 (Z8)		C2(Z9)		C19(Z150)		C8 (Z75)	C8 (Z78)		C9 (Z102)		C9 (Z120)		C15 (Z145)		C15 (Z146)		C8 (Z70)		C8 (Z74)	
Textural Part	n	d	n	d	n	d	n	ns	on	ns	on	n	on	n	on	n	on	oc	or	oc	or
$Si O_2$	0.00	0.00	0.00	0.00	0.00	0.00	0.00	0.00	0.00	0.13	0.25	0.00	0.00	0.05		0.13	0.18	0.00	0.00	0.00	0.00
$Ti O_2$	0.18	0.16	0.11	0.10	0.23	0.17	0.31	0.26	0.26	0.36	0.18	0.39	0.00	0.11		0.16	0.19	0.30	0.18	0.46	0.00
$Al_2 O_3$	7.95	8.14	8.86	8.58	11.29	11.11	19.08	14.50	14.53	14.83	14.35	18.19	17.61	14.59		14.61	15.34	18.53	17.83	19.13	18.71
$Cr_2 O_3$	64.10	62.56	61.83	61.11	59.63	59.52	51.43	54.74	54.23	54.30	53.90	51.47	51.02	53.80		55.04	53.72	51.08	51.49	50.31	49.73
$V_2 O_3$	0.00	0.00	0.09	0.08	0.00	0.15	0.35	0.09	0.10	0.27	0.22	0.24	0.00	0.12		0.19	0.29	0.23	0.22	0.00	0.00
$Fe_2 O_3$ *	2.81	3.47	2.56	2.32	3.24	2.48	2.00	3.31	2.82	2.78	3.40	4.23	5.42	3.84		3.77	2.85	2.58	1.23	3.66	4.54
Fe O *	11.72	13.85	10.63	12.87	11.42	13.18	11.87	11.74	13.75	14.28	16.53	10.79	11.95	12.27		12.69	13.58	16.09	19.11	12.45	14.09
Mg O	14.36	13.00	13.87	12.13	14.62	13.41	14.79	14.20	12.85	13.02	11.52	15.94	14.85	13.83		14.22	13.35	12.71	10.11	14.72	13.56
Mn O	0.00	0.00	0.77	0.85	0.34	0.23	0.71	0.69	0.68	0.28	0.40	0.10	0.31	0.66		0.25	0.57	b.d.	0.36	0.64	0.48
Ca O	0.00	0.00	0.01	0.01	0.00	0.00	0.00	0.05	0.01	0.00	0.00	0.00	0.00	0.01		0.00	0.00	0.00	0.00	0.00	0.00
Ni O	0.00	0.00	0.42	0.43	0.00	0.00	0.16	n.d.	n.d.	0.22	0.13	0.11	0.12	n.d.		n.d.	0.06	b.d.	0.25	0.00	0.00
Co O	0.00	0.00	0.10	0.06	0.00	0.00	0.00	0.07	0.08	0.00	0.12	0.11	0.13	0.04		0.00	0.00	0.00	0.00	0.00	0.00
Total	101.12	101.18	99.25	98.54	100.77	100.25	100.70	99.65	99.31	100.47	101.00	101.57	101.41	99.32		101.18	100.13	101.52	100.78	101.37	101.11
Cr / Fe ***	3.960	3.246	4.210	3.598	3.664	3.400	3.312	3.276	2.930	2.848	2.423	3.105	2.668	3.010		3.014	2.928	2.442	2.243	2.812	2.410
100 $Mg/(Mg+Fe^{2+})$	68.585	62.593	69.925	62.678	69.527	64.457	68.958	68.317	62.468	61.901	55.390	72.481	68.879	66.760		66.641	63.662	58.478	48.516	67.811	63.176
100 Cr/(Cr+Al)	84.396	83.782	82.386	82.686	77.983	78.234	64.389	71.682	71.446	71.065	71.581	65.484	66.022	71.206		71.647	70.130	64.892	65.944	63.809	64.058
Analyses of olivine grains adjacent to respective chromite grains :																					
$Si O_2$	41.83	41.19		40.82		41.30		43.29	42.98	40.75	40.73	41.62	41.41	42.45	42.47	41.73	42.58	41.59	41.55		
Fe O **	4.43	4.91		5.57		4.47		3.11	4.93	5.65	7.26	4.47	4.78	4.05	5.35	4.37	5.89	8.09	7.58		
Mg O	53.00	52.48		52.25		52.17		52.62	51.02	51.50	50.38	53.44	53.11	52.56	51.19	54.40	50.59	48.99	49.13		
Mn O	0.17	0.13		b.d.		b.d.		b.d.	b.d.	0.11	0.19	0.09	0.11	b.d.	b.d.	0.14	b.d.	0.21	0.17		
Ca O	0.12	0.09		0.07		n.d.		0.00	0.05	0.10	0.03	0.17	0.09	b.d.	0.02	0.01	0.00	b.d.	b.d.		
Ni O	0.68	0.50		0.42		0.59		n.d.	n.d.	0.58	0.47	0.40	0.47	n.d.	n.d.	0.54	n.d.	0.52	0.52		
Total	100.23	99.30		99.13		98.53		99.02	98.98	98.69	99.06	100.19	99.97	99.06	99.03	101.19	99.06	99.40	98.95		
Fo (/)	95.354	94.887		94.367		95.406		96.791	94.868	94.174	92.509	95.434	95.098	95.870	94.459	95.527	93.869	91.543	92.047		

Deposit numbers refer to fig.1. Sp.No.= Sample number. n.d. = Not determined. b.d. = Below detection limit.
* = Calculated from total iron assuming RO:R_2O_3 ratio of 1 : 1. ** = Total Fe as Fe O. *** = Ratio from weight percentages.
d = Disseminated chromite outside the nodules of porphyritic nodular ores. n = Coarse nodules. ns = Silicate rich nodules.
on = Outside the nodules but adjacent. oc = Orbicule centre. or = Orbicule rim.

contents but not in Cr, Al, or Fe^{3+}. The nodules possess higher $Mg(Mg/(Mg+Fe^{2+}) > 0.65)$, and lower Fe than the chromite in the disseminated chromitite part $(Mg/(Mg+Fe^{2+}) < 0.65)$. This relationship is noticeable for samples with well-sorted nodules, e.g. Z8 and Z9 from C2 deposit (Table I) and also for those with poorly sorted nodules, such as Z150 from C19 illustrated in fig. 2F. In the latter case, analyses from finer and coarser nodules are similar. In some samples from C2, the matrix is partly dunite, partly disseminated chromitite, but the nodules in both parts have similar compositions.

The orbicular ore photograph (fig. 2D) shows different chromite : silicate ratios for the orbicule 'nuclei' and 'rims'. Analyses of associated nucleus-, rim-chromite pairs (Table I) show similar Cr, Al, and Fe^{3+} contents with higher Fe^{2+} for the 'rims' and higher MgO for the 'nuclei'. As the orbicule 'nuclei' alone look like the nodules of nearby nodular ores in the same deposit (C8), and are unzoned, analyses from both are given in Table I for comparison. The sample with solid nodules (Z75) has broadly similar Cr, Al, lower total Fe, and higher MgO compared to the orbicule 'nuclei'. The sample with silicate-rich nodules (Z78) has lower Al and higher Cr contents.

The 'normal' nodular ores from nearby but discrete ore bodies at C8 deposit, representing various nodule sizes and closeness of packing, did not reveal a regular variation. The fewer grains of fine chromite in the olivine matrix possess lower Mg and higher Fe than the nodule-making coarser chromite.

The Fo content of olivines in nodular ores ranges from 91.4 to 96.8%, with highest frequency around 95%. These values resemble those of olivines from non-nodular chromitites of the same district. Some representative olivine analyses are listed in Table I. In individual samples the olivines within the chromite nodules possess higher Fo contents than those from just outside the nodules. In porphyritic nodular ores, the Fo range is 94.4 to 95.5%. In orbicular ores, the olivines in the orbicule 'mantles' (Fo 90.9-91.6%) and 'rims' (Fo 91.1-92.2%) do not show large or consistent differences.

Discussion

The nodular texture is a critical feature of podiform deposits (Thayer, 1960, 1969; Dickey, 1975; Greenbaum, 1977) and its formation requires conditions obtainable only in the alpine-type environments, in view of its complete absence in the stratiform complexes. Thus, with a few exceptions (e.g. Zengin, 1961), most researchers support a deep-seated magmatic origin for the nodular ores. The mechanisms proposed include:

(i) Gravitational segregation and accretion of chromite grains, and their rounding and rolling along steeper (dip $\geqslant 25°$) layers (Borchert, 1961).

(ii) Nodule formation as droplets of chromite-rich and chromite-poor immiscible liquids (Shams, 1964; Bilgrami, 1964; Pavlov *et al.*, 1977).

(iii) Rounding of nodules by abrasion and, or, resolution (Ramp, 1957; Kaaden, 1970), and resorption and hydrothermal attack.

(iv) 'Snowballing' in a turbulent zone of magma segregation (Dickey, 1975).

(v) Crystallization from a system undercooled and, or, supersaturated in Cr forms dendritic growths of chromite. Their infilling and overgrowth in 'metastable' conditions results in nodules (Greenbaum, 1977; Leblanc, 1980). This mechanism is based on observations from the Troodos complex only, where the dendritic texture is developed within, as well as between the nodules. Such dendritic texture is not reported from other places, and is absent in the Sakhakot-Qila chromitites.

(vi) Chromite pelletization by elutriation in parts of magmatic pipes where its downward motion is in dynamic equilibrium with upward fluid pressure (Cassard *et al.*, 1981).

(vii) Orthomagmatic growth of nodules while freely suspended in magma, and by very slow cooling; and subsequent gravitational crystal settling without compaction or deformation under load (Johnston, 1936; Thayer, 1969). The pure chromite rims of cored nodules indicate a gradual shift in equilibrium. The views of Thayer (1969) are also supported by the evidence from Sakhakot-Qila chromitites presented here.

The segregation of chromite has been cited as prima-facie evidence of crystal settling from fluid magma (Thayer, 1970), and the chromitites often display textures regarded as cumulate. A wide distribution of such textures in the Sakhakot-Qila chromitites is evident from fig. 1. These textures in podiform chromitites indicate magmatic crystal settling in primary environments (Thayer, 1969). Nodular ores at Sakhakot-Qila occur adjacent to such cumulate-textured ores. Moreover, the chromite compositions at various deposits show similar values for Cr and Al contents for both the nodular and non-nodular ores. The variations in Cr and Al contents in different stratigraphic subzones are similar for nodular and non-nodular chromitites, and probably had a common control, and cumulus origin.

The porphyritic nodular texture has not been recognized earlier, and this fabric, as shown in fig. 2F, indicates that both the nodules and the finer disseminated chrome ores may have been produced by the same processes and have crystallized from magmatic liquids of roughly the same composition and chromite : silicate ratio as those responsible for the formation of non-nodular chromitites. The variously sized nodules at C19 (fig. 2F) may have suffered *en masse* movement before maturity to more uniform sizes. However, such large variations in nodule sizes are absent in most discrete bodies of nodular ores at this complex, and the nodule sizes in them are fairly uniform. Such ores may be related to the latter stages of nodule formation. The idea of a Cr-rich immiscible liquid parent of the nodules (Shams, 1964) lacks supporting evidence for the existence of such liquidus compositions in the studied experimental systems. The system MgO–Cr_2O_3–SiO_2 (Keith, 1954) includes a prominent field of liquid immiscibility, but the high temperatures and the compositions for immiscibility are unlike those of natural magmas. The porphyritic nodular texture does not favour the liquid immiscibility mechanism for nodular chromitites because the nodule-forming and the matrix-forming parts are both chromite-rich, contrary to the Cr-rich and Cr-poor immiscible liquid fractions proposed so far for nodular textures.

Deer *et al.* (1962) have mentioned the evidence from certain podiform deposits that chromites of later stages are enriched in Mg and Al. Moreover, in the Sakhakot–Qila complex, it appears that the variation in the Cr : Al ratios of chromites are caused by fractional crystallization of magmas at different temperatures, as there is no plagioclase to counter this trend (Dickey, 1975). The porphyritic nodular ores probably formed prior to the more typical nodular and orbicular ores, as is suggested by its lowest stratigraphic position and highest Cr/Al ratio (figs. 1 and 3A).

The origin of orbicular ore has usually been explained by chromite precipitation to form nodules which serve as nuclei for olivine. Finally interstitial (postcumulus) chromite crystallizes by reversal of equilibrium (Thayer, 1969). According to Greenbaum (1977), orbicules are mechanical concretions formed by accretion of settled chromite and olivine about a nucleus of dunite due to gravitational rolling along slumps in crystal mush, or by oscillatory bottom currents in the magma. The association of nodular and orbicular ores at the neighbouring locations at C8 suggests that both can form from magmas of similar composition. Both occur enclosed in one dunite body. The SEM observations of Leblanc (1980) on chromite crystals show that chromite nodules and orbicules have similar surfaces. The growth of nodules as nuclei in the cell centres of chromite nets (fig. 2D) probably reflects a close genetic link, and is supported by the close spatial association of nodular and chromite-net textures at C8 and C53.

Thus, the evidence points towards similarity in the genesis of nodular, orbicular, and porphyritic nodular ores, their formation by cumulus processes, and growth while freely suspended in magma (Thayer, 1969). The compositions of such ores from various deposits are shown in a $Cr/(Cr+Al)$ *vs.* $Mg/(Mg+Fe^{2+})$ plot in fig. 3. The points fall in the area of alpine-type chromitites (Irvine, 1965, 1967), and show a strong Cr–Al variation with very small Mg–Fe^{2+} variation. However, to avoid the effects of subsolidus re-equilibration, if only the coarse, nodule-forming chromites are considered, the trend is unusual, as it exhibits a slight sympathetic variation. This relationship is incompatible with the generally reported trend in alpine-type ultramafic rocks, where a decrease in $Cr/(Cr+Al)$ accompanies an increase in $Mg/(Mg+Fe^{2+})$ (Irvine, 1967; Evans and Frost, 1975; Henderson, 1975; Malpas and Strong, 1975; Medaris, 1975; Leblanc *et al.*, 1980; Cassard *et al.*, 1981), and some unrecrystallized stratiform intrusions (Hamlyn and Keays, 1979). It also deviates from the trend obtained in the Sakhakot–Qila chromitites without discriminating between nodular and non-nodular ores (fig. 3B). Thus, it is suggested that the trend reflects the differences in the magmatic compositions. A trend of decreasing Cr_2O_3 with MgO and Al_2O_3 was also observed by Evans and Wright (1972) from the liquidus chromite of Kilauea volcano, Hawaii. Oen *et al.* (1979), in chromites of different deposits in the Ni arsenide-bearing chromitites of Malaga, Spain, found a similar relationship to the parent magmatic compositions, rather than to later recrystallization and re-equilibration. Chromitites are very rare as nodules in the basaltic or kimberlitic rocks, and are probably absent in the lherzolitic upper mantle (Arai, 1978). Lherzolitic xenoliths in basalts are characterized by highly aluminous chromite (e.g. Basu and MacGregor, 1975). However, the nodular chromitite found as nodules in alkali olivine basalt consists of lherzolitic matrix around the nodules of chromite with highly Cr-rich ($Cr/R^{3+} = 0.78$) and Mg-rich composition (Arai, 1978).

The trend of compositional variation for non-nodular chromitites is different from that of the nodular chromitites. These start crystallizing as Cr-rich chromites in the more basal zones, but successive phases crystallize chromites in which the Al-enrichment and Cr-depletion is accompanied by consistent but slight increase in Mg.

The spherical shapes of the nodules may also be

considered as one extreme of the general trend of chromite crystals to have euhedral forms in stratiform deposits which crystallize in the upper crust, and to develop subspherical forms with rounded edges in podiform deposits generated at deeper levels (Thayer, 1970; Leblanc, 1980). The nodules are not always typically spherical and may display, in some cases, external forms intermediate between typical nodules and large 'crystals' (e.g. Thayer, 1969, fig. 7; Leblanc, 1980, fig. 2c). At spreading ridges, the generation of podiform chromitites may accompany the uprising of host ultramafic mass in several steps and at various levels. It seems probable that the nodules start crystallizing by very slow cooling in small discrete pods or layers of molten material when the ultramafic mass is at deeper levels. Its progressive rise leads to crystallization of finer-sized nodules, and then towards non-nodular ores. The finer chromite grains crystallize relatively later, but from the same magma layer or pocket that forms the associated nodules. Thus, the nodular and associated non-nodular chromites at each deposit have similar trivalent metal contents. Initially, the layers and pods of chromitites and enveloping dunites were probably interconnected as they passed through an earlier magmatic differentiation producing the stratigraphic Cr–Al variations of these chromites. The Mg–Fe variations in chromite grains within each deposit, or sample, parallel its relative grain size. The coarser grains of chromite are Mg-rich relative to fine grains which are Fe-rich. However, there is no regular variation of trivalent metals with grain size.

Geothermometry

Geothermometric methods based on Mg–Fe exchange between the coexisting olivine and chromian spinel have received considerable attention (e.g. Irvine, 1965, 1967; Jackson, 1969; Evans and Frost, 1975; Fujii, 1977; Mori, 1977; Roeder *et al.*, 1979; Fabries, 1979) and have been applied to the petrogenesis of many ultramafic complexes (e.g. Henry and Medaris, 1980; Himmelberg and Loney, 1980; Fabries, 1979; Hamlyn, 1980; Jan and Howie, 1981). In natural occurrences the different proposed calibrations yield slightly different absolute values of temperature but some workers have stressed that the methods are more accurate when used in a relative sense (Irvine, 1965; Jackson, 1969; Roeder *et al.*, 1979). The temperatures calculated for many alpine-type peridotites using the recent versions of the olivine–spinel geothermometer show that the olivine and chromian spinel continue to equilibrate at quite low temperatures, most frequently to about 700 °C (Evans and Frost, 1975; Medaris, 1975; Fabries, 1979; Arai, 1980) and similar values are reported for ultrabasic stratiform intrusions as well (e.g. Hamlyn, 1980), whereas the pyroxenes stop equilibrating with olivine and spinel at higher temperatures (Henry and Medaris, 1980). However, many ultrabasic complexes are known where the olivine–spinel exchange also seems to have stopped at higher temperatures (Jackson, 1969; Hamlyn, 1980; Clark, 1978; Jan and Howie, 1981). For the Sakhakot-Qila nodular ores, the final temperatures of olivine–spinel equilibration lie between 750 and 900 °C, as shown in fig. 4 which plots the compositions of coexisting grains in different textural units of the samples of nodular and related ores, and compares them with the proposed isotherms from Evans and Frost (1975). $\ln K_D^*$ represents the logarithm of the partition coefficient calculated on the basis of constant Fe^{3+} content, as defined by Evans and Frost (1975). An isothermic straight-line relationship is not clear from the plot of nodular ores only, but a less dispersed and linear relationship is obtained when the analyses from non-nodular chromitites, especially those with Al-rich chromites, are also plotted. In fig. 5 the temperatures calculated by two of the proposed formulations are given for various kinds of chromite grains to observe their relative differences. Fabries's (1979) method gives higher temperatures than those from the method of Roeder *et al.* (1979) by amounts ranging from 70 to 140 °C. It appears that in individual chromite samples the textural units identified by the relative

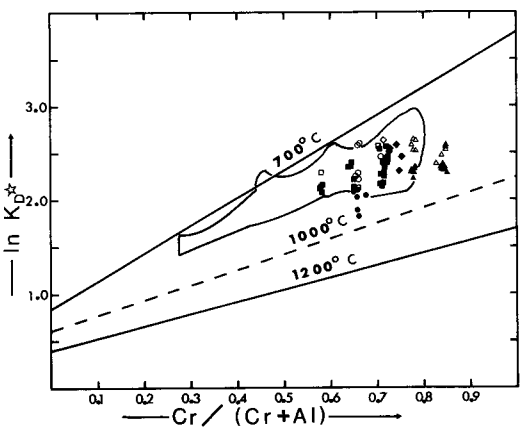

FIG. 4. Olivine–spinel geothermometric plot of the nodular and related ores of the Sakhakot-Qila complex, after Evans and Frost (1975). Cr/(Cr + Al) in chromite is plotted against $\ln K_D^*$ (i.e. $\ln K_D$Mg-Fe^{2+} normalized to $Y^{SP}_{Fe^{3+}} = 0.05$). Different symbols represent different types of chromite grains as listed in fig. 3(A). The field of non-nodular segregated chromite is plotted for comparison.

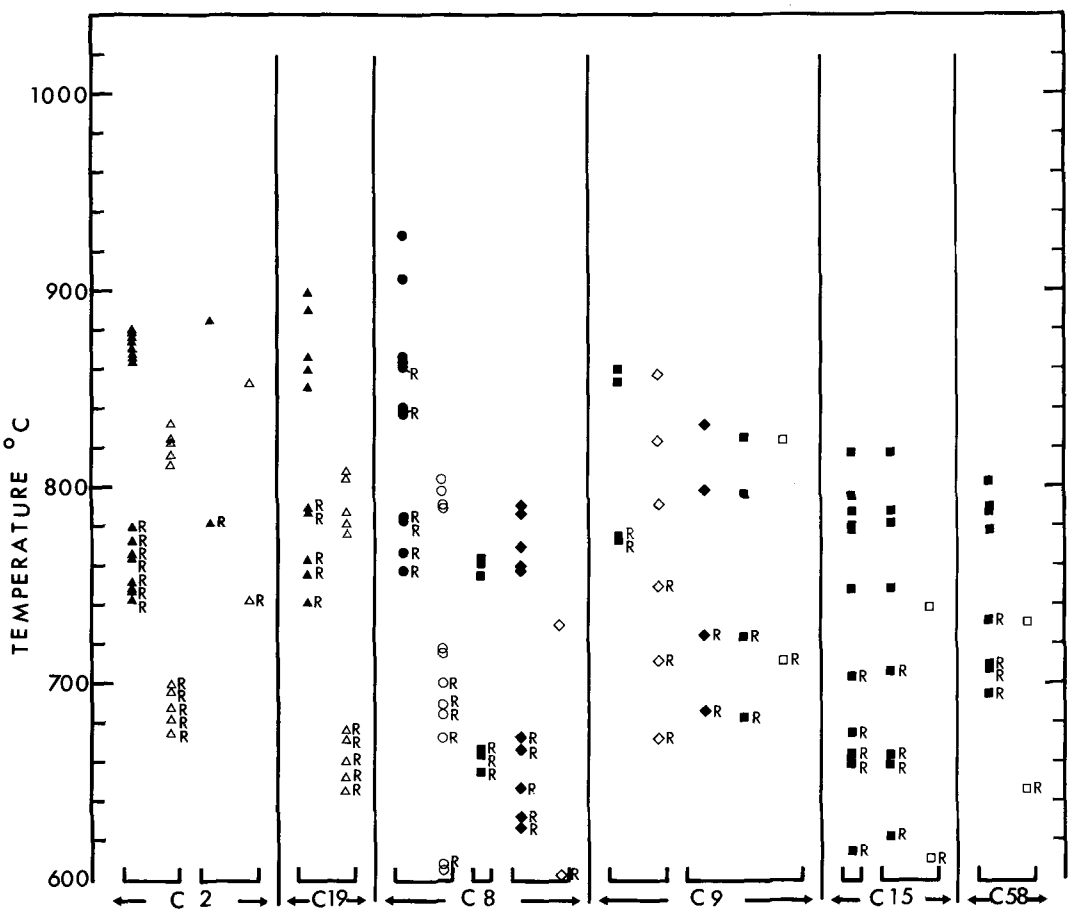

FIG. 5. Equilibration temperatures of olivines and different types of adjacent chromite grains of nodular and related ores, calculated using formulations by Fabriés (1979) and Roeder *et al.* (1979). The latter are indicated by the letter 'R'. Textural symbols are similar to those in fig. 3(A). Deposit numbers are written on the base line, and each bracket encloses one sample or adjacent samples.

chromite grain sizes and, or, chromite: silicate ratios behaved independently as a closed system during the final leg of their subsolidus re-equilibration, probably because of restricted diffusion. Figs. 4 and 5 show that temperatures of final equilibration are higher for the nodule-forming coarser chromite grains, shown by solid symbols, than those for the finer chromite grains outside the nodules, shown by open symbols. In the porphyritic nodular ores, the matrix chromitite part has equilibrated 50–80 °C below the coarser nodules whose temperature based on Fabries's (1979) equation range from 830 to 890 °C. In the orbicular ore, the solid chromite 'nuclei' exhibit temperatures of 838–929 °C, compared to 716–805 °C range from the orbicule rims. It seems probable that relatively earlier crystallized fractions stop equilibrating with the adjacent olivines at slightly higher temperatures. Thus, in the orbicular ores, the chromite of orbicule 'nuclei' stopped equilibrating with the surrounding olivine at relatively higher temperatures than the chromite in the orbicule 'rims' as well as that in the associated nodular chromitites. Similarly, the porphyritic nodular ores which show higher temperatures of final equilibration than the nodular ores, also occur at the lower stratigraphic levels of the chromitiferous zone of the complex, and have higher Cr/(Cr + Al) ratios of their chromites, suggesting an earlier crystallization. The experimental evidence (Dickey and Yoder, 1972) also shows that the spinels in equilibrium with silicate melts and clinopyroxene

become more chromian with increasing temperature.

Conclusions

The porphyritic nodular texture as described here invalidates some earlier suggestions that certain special conditions, i.e. the existence of undercooled and, or, supersaturated fluids, or immiscible liquids, are essential for the formation of the nodular texture which is a characteristic feature of the alpine-type chromitites. Although many aspects of the process of nodule formation still remain to be explained, the Sakhakot-Qila chromitites show that it results from deep-seated cumulate processes, by very slow orthomagmatic crystal growth. The associated cumulate textures and a stratigraphical variation of chromite composition, and chromitite textures goes against the origin of these chromitites as refractory residues (cf. Arai, 1980). The nodular and orbicular ores occur side by side and seem to be genetically related. The composition of nodular chromites at initial magmatic stages, judging from their trivalent metal (Al, Cr) contents is comparable to that of the chromites showing non-nodular cumulate textures and occurring besides nodular ores at individual deposits. Moreover, there is similarity of stratigraphic variation of chromite compositions which, in nodular and non-nodular ores alike, show high-Cr chromites in southern deposits and high-Al chromites in northern deposits. However, the spinel compositional prism (fig. 3) shows a trend which may be distinctive for nodular chromites. The effects of postmagmatic and subsolidus re-equilibration between chromite and olivine are reflected in the enrichment in Mg cation fraction of the chromitite parts with coarser chromite grains and higher modal chromite in both the chromite and olivine structures (Clark, 1978).

The nominal temperatures of the cessation of such re-equilibration obtained from olivine-spinel geothermometry range from about 930 °C down to the lowest value of about 760 °C for these chromitites. Apparently, this re-equilibration was not effected by any subsequent events such as metamorphic recrystallization. The nodule-forming chromites stop equilibrating with adjacent olivine grains at slightly higher temperatures than the chromite grains outside the nodules.

Acknowledgements. This work was carried out under the academic guidance of Professor R. A. Howie and supervision of Dr A. Hall. The electron-probe analyses were performed at University College London, and Dr R. M. F. Preston and Mr Ian Young are thanked for assistance. Financial support was provided by the Government of Pakistan.

REFERENCES

Ahmed, Z., and Hall, A. (1981) *Chem. Erde*, **40,** 209–39.
Arai, S. (1978) *Rep. Fac. Sci. Shizuoka Univ.* **12,** 99–113.
——(1980) *J. Petrol.* **21,** 141–65.
Basu, A. R., and MacGregor, I. D. (1975) *Geochim. Cosmochim. Acta*, **39,** 937–45.
Bilgrami, S. A. (1964) *Rec. Geol. Surv. Pakistan* **10** (2C), 1–28.
Borchert, H. (1961) *CENTO Symp. Chrome Ore, Ankara*, 92–107.
Cassard, D., Rabinovitch, M., Nicolas, A., Moutte, J., Leblanc, M., and Prinzhofer, A. (1981) *Econ. Geol.* **76,** 805–31.
Clark, T. (1978) *Can. J. Earth Sci.* **15,** 1893–1903.
Deer, W. A., Howie, R. A., and Zussman, J. (1962) *Rock Forming Minerals*, vol. 5, Longmans, London.
Dickey, J. S., *Jr.* (1975) *Geochim. Cosmochim. Acta*, **39,** 1061–74.
—— and Yoder, H. S., *Jr.* (1972) *Carnegie Inst. Washington Yearb.* **71,** 384–92.
Evans, B. W., and Frost, B. R. (1975) *Geochim. Cosmochim. Acta*, **39,** 959–72.
—— and Wright, T. L. (1972) *Am. Mineral.* **57,** 217–30.
Fabries, J. (1979) *Contrib. Mineral. Petrol.* **69,** 329–36.
Fujii, T. (1977) *Carnegie Inst. Washington Yearb.* **76,** 563–9.
Greenbaum, D. (1977) *Econ. Geol.* **72,** 1175–93.
Hamlyn, P. R. (1980) *Am. J. Sci.* **280,** 631–8.
—— and Keays, R. R. (1979) *Contrib. Mineral. Petrol.* **69,** 75–82.
Henderson, P. (1975) *Geochim. Cosmochim. Acta*, **39,** 1035–44.
Henry, D. J., and Medaris, L. G., *Jr.* (1980) *Am. J. Sci.* **280**-A (the Jackson Volume), 211–31.
Himmelberg, G. R., and Loney, R. A. (1980) Ibid. **280**-A, 232–68.
Irvine, T. N. (1965) *Can. J. Earth Sci.* **2,** 648–72.
——(1967) Ibid. **4,** 71–103.
Jackson, E. D. (1969) In *Magmatic Ore Deposits* (Wilson, H. D. B., ed.), Econ. Geol. Mon. 4, 41–71.
—— and Thayer, T. P. (1972) *Proc. 24th Int. Geol. Congr.* **2,** 289–96.
Jan, M. Q., and Howie, R. A. (1981) *J. Petrol.* **22,** 85–126.
Johnston, W. D., *Jr.* (1936) *Econ. Geol.* **31,** 417–27.
Kaaden, G. v. d. (1963) *Bull. Min. Res. Expl. Inst. Turkey*, **61,** 41–56.
——(1970) *Spec. Publ. Geol. Soc. S. Africa*, **1,** 511–31.
Keith, M. L. (1954) *J. Am. Ceram. Soc.* **37,** 490–6.
Leblanc, M. (1980) *Mineral. Dep.* **15,** 201–10.
—— Cassard, D., and Juteau, T. (1981) Ibid. **16,** 269–82.
Malpas, J., and Strong, D. F. (1975) *Geochim. Cosmochim. Acta*, **39,** 1045–60.
Medaris, L. G., *Jr.* (1975) Ibid. **39,** 947–58.
Mori, T. (1977) *Contrib. Mineral. Petrol.* **59,** 261–79.
Mukherjee, S. (1969) *Econ. Geol.* **64,** 329–37.
Oen, I. S., Kieft, C., and Westerhof, A. B. (1979) Ibid. **74,** 1630–6.
Pavlov, N. V., Grigor'yeva, I. I., and Tsepin, A. I. (1977) *Int. Geol. Rev.* **19** (1), 43–56.
Ramp, L. (1957) *Min. Engrg.* 894–7.
Roeder, P. L., Campbell, I. H., and Jamieson, H. E. (1979) *Contrib. Mineral. Petrol.* **68,** 325–34.

Shams, F. A. (1964) *Econ. Geol.* **59,** 1343–7.
Snelgrove, A. K., and Ruotsala, A. P. (1968) *Geol. Bull. Punjab Univ.* **7,** 31–42.
Stevens, R. E. (1944) *Am. Mineral.* **29,** 1–34.
Thayer, T. P. (1960) *Proc. 21st Int. Geol. Congr. Copenhagen,* **13,** 247–59.
——(1964) *Econ. Geol.* **59,** 1497–524.
——(1969) In *Magmatic Ore Deposits* (Wilson, H. D. B., ed.), Econ. Geol. Mon. 4, 132–46.
——(1970) *Spec. Publ. Geol. Soc. S. Africa,* **1,** 380–90.
Zengin, Y. (1961) *CENTO Symp. Chrome Ore, Ankara,* 122–9.